CLASSIFICATION CANCELED

RESTRICTED

TECHNICAL NOTES

NATIONAL ADVISORY COMMITTEE FOR AERONAUTICS

No. 908

FOR REFERENCE

SOME INVESTIGATIONS OF THE GENERAL INSTABILITY

OF STIFFENED METAL CYLINDERS

IV - CONTINUATION OF TESTS OF SHEET-COVERED SPECIMENS

AND STUDIES OF THE BUCKLING PHENOMENA

OF UNSTIFFENED CIRCULAR CYLINDERS

Guggenheim Aeronautical Laboratory
California Institute of Technology

Washington
August 1943

NATIONAL ADVISORY COMMITTEE FOR AERONAUTICS

TECHNICAL NOTE NO. 908

SOME INVESTIGATIONS OF THE GENERAL INSTABILITY

OF STIFFENED METAL CYLINDERS

IV - CONTINUATION OF TESTS OF SHEET-COVERED SPECIMENS

AND STUDIES OF THE BUCKLING PHENOMENA

OF UNSTIFFENED CIRCULAR CYLINDERS

Guggenheim Aeronautical Laboratory
California Institute of Technology

This is the fourth of a series of reports
covering an investigation of the general
instability problem by the California
Institute of Technology. The first five
reports of this series cover investiga-
tions of the general instability problem
under the loading conditions of pure bend-
ing and were prepared under the sponsor-
ship of the Civil Aeronautics Administra-
tion. The succeeding reports of this
series cover the work done on other load-
ing conditions under the sponsorship of
the National Advisory Committee for Aero-
nautics.

INTRODUCTION

This report is to deal primarily with the continua-
tion of tests of sheet-covered specimens and studies of
the buckling phenomena of unstiffened circular cylinders.
The earlier work on this investigation of the problem of
general instability of stiffened metal cylinders at C.I.T.
has been reported in references 1, 2, and 3. Tests have
been completed on the first series of sheet-covered spec-
imens. The longitudinals and frames of the sheet-covered
specimens were identical to those of the wire-braced spec-
imens discussed in reference 3. The sheet covering was
in all cases 0.010-inch 17S-T dural. The longitudinal
spacing was varied from 2.53 to 10.12 inches and the
frame spacing from 1 to 16 inches. An attempt has been

made to correlate the experimental data of the wire-braced
and sheet-covered specimens. A detailed discussion is
given in the discussion of the normal restraint coefficient
in this report. Ryder's theoretical work has been applied
to three specimens. The results are tabulated in table
III and discussed in the body of the report.

In addition to the results on the sheet-covered spec-
imens, the results of an investigation on axially loaded
thin-wall metal cylinders will be included in this report.
As the preliminary work of this investigation was dis-
cussed in reference 2, only results of the more recent
work are included. An important finding of this investi-
gation has been the determination of the initial wave form.
It has been found that the initial wave form does not agree
with the uniform sinusoidal type of wave which has been
previously assumed for the theoretical solution, but is
elliptical in shape, scattered at random through the cyl-
inder, and changes to a diamond shape as the load is in-
creased.

EXPERIMENTAL INVESTIGATION OF SHEET-COVERED SPECIMENS

As pointed out in reference 2, a number of sheet-
covered specimens were to be tested to determine whether
or not a correlation could be obtained between the fail-
ing bending moments of the wire-braced and the sheet-
covered specimens. The construction of the sheet-covered
and wire-braced specimens was essentially similar, the
only difference being that the wire bracing was replaced
by the sheet. Details of construction and test procedure
have been discussed in detail in reference 2 and will not
be repeated here.

Table I gives the complete set of sheet-covered spec-
imens which have been tested, the number of frames and
longitudinals in each specimen, the failing bending mo-
ment, the critical compressive longitudinal stress, and
the restraint coefficient. Specimens 25 to 28 were dis-
cussed in reference 3, and specimens 29 to 39 have been
tested since that report was written.

Specimen 29 failed by panel instability; the tabulat-
ed compressive stress is that at which buckling between
frames started and corresponds to a moment of 66,000 inch-
pounds. Because of the symmetrical buckling of the lon-
gitudinals, transverse stresses were set up in the sheet.

As the amplitudes of the longitudinals increased, the
transverse stresses became larger and the stabilizing ef-
fect of the sheet increased. This stabilizing effect of
the sheet on the longitudinals was quite evident at the
higher loads, as illustrated in figures 2 and 38, and pre-
vented collapsing of the specimen. The bending moment
was increased to 123,000 inch-pounds without any definite
failure. Specimens 28 and 34 started to fail by panel in-
stability; however, upon increasing the bending moment the
frames failed at the tabulated bending moment. The loads
at which panel instability occurred were 140,000 and 45,000
inch-pounds, respectively.

In figure 4 the compressive failing stress, which is
discussed later, is plotted as a function of the longitudi-
nal spacing b, for constant values of d/b, referred to
as "aspect ratio." It is of considerable interest to note
that each curve is displaced by a contraction or expansion
of the abscissa. The regularity of this family of curves
would indicate that such a parameter exists that if the
compressive stress is plotted as a function of this param-
eter a single curve would be obtained. If such a param-
eter can be found, a limiting value could be established
which would indicate the transition region between panel
instability and general instability. A number of parame-
ters have been attempted, but as yet the results have not
been very successful. In figure 37 the failing compres-

sive stress has been plotted as a function of $\sqrt[3]{\dfrac{I_{\sigma_f}}{d}\dfrac{I_{\sigma_l}}{b}}$

the parameter suggested by Dschou's work. (See reference
1, p. 12). The resulting curve indicates a linear rela-
tionship.

In calculating I_{σ_l} and I_{σ_f}, the following assump-
tions were made:

1. The effective width of sheet acting with each
longitudinal can be calculated by Marguerre's equation,

$$\frac{w_e}{b} = \frac{1}{2}\sqrt{\frac{\sigma_l}{\sigma}}$$

where

σ_l longitudinal stress

σ_b buckling stress of sheet

2. The effective width of sheet acting with the frame is equal to the effective width of sheet acting with the longitudinal.

I_{σ_l} is then the moment of inertia of the longitudinal plus an effective width of sheet corresponding to the longitudinal stress σ, and I_{σ_f} is the moment of inertia of the frame plus an effective width of sheet equal to that acting with the longitudinal. In view of these rather arbitrary assumptions, too much confidence should not be placed in this curve until further investigations have been carried out on the effects of changing the sheet thickness, and the stiffness of the frames and the longitudinals.

Ryder's analysis could be applied only to three specimens: namely, 25, 26, and 27, as the parameters of the other specimens lie outside the range covered by the published charts. The results for these three specimens are given in table III. In all three cases the calculated panel instability stress is larger than the calculated general instability stress; hence the method predicted correctly the occurrence of general instability. The predicted instability stress and the experimental value are in good agreement for specimen 27; for specimens 25 and 26 the predicted stresses are considerably lower than the experimental stresses.

An extensive comparison between the theoretically predicted general instability stresses and the experimentally obtained stresses will be given after tests have been conducted on specimens in which the sheet thickness and the stiffness of the frames and the longitudinals have been varied.

MAXIMUM STRESSES IN THE LONGITUDINALS

In the first sheet-covered specimens an attempt was made to measure the stresses in the longitudinals with Huggenberger extensometers. The stress measurements as indicated by the curves in figures 13 to 16 have not been very successful. Various methods of attaching the instruments to the longitudinals have been tried; however, the irregularity of the stress measurements has not been eliminated. A method of measuring the maximum stresses which has been adopted is to measure the over-all maximum

deflections of the specimen by means of dial gages, as
shown in the photographs (figs. 3 and 38 to 47). If the
elastic modulus of the longitudinals and the over—all
strain are known, the stresses can be calculated. Since
the radial deflections of the stiffeners are measured for
various increments of load, the maximum stress can be
correctly calculated, even for cases in which radial de-
flection occurs, by means of the equation

$$\sigma = \frac{\Delta L E}{L} - \frac{E}{2L} \int_0^L \left(\frac{\partial w}{\partial x}\right)^2 dx$$

where

σ stress, pounds per square inch

ΔL total over—all deflection, inches

L length of the specimen, inches

w radial deflection, inches

The expression $\frac{E}{2L} \int_0^L \left(\frac{\partial w}{\partial x}\right)^2 dx$ is the correction for the
deflection caused by the wave form of the longitudinals.
It has been found that, in general, the correction due
to the curvature (M/EI) is quite small; however, for
cases in which the longitudinals buckle between frames,
the correction becomes quite appreciable. These correc-
tions were made in the measured over—all deflections of
specimen 34. The results of this latter type of stress
measurement are shown in figures 8 to 12, in which the
stress is plotted as a function of the applied bending
moment. It is felt that these results are more reliable
than those obtained from the extensometer readings. One
disadvantage is that only the maximum stresses are measured;
however, in the majority of cases only the maximum stresses
are of primary importance.

The compressive stress curve in figure 12 is rather
interesting in that three definite breaks occur in the
curve. It seems logical to assume that the first break
is due to buckling of the sheet between longitudinals,

the second to buckling of the sheet between rivets, and
the third to the stress exceeding the proportional limit
of the material.

A new method of calculating the actual stress which
occurs in the longitudinals of stiffened cylinders sub-
jected to pure bending has been recently developed by
H. L. Cox (reference 4). Stress calculations based on
this method are in excellent agreement with the above-
described measured stresses. The tabulated stresses for
specimens 25, 26, and 28 were not measured but merely cal-
culated by this method; the stress for specimen 28 was
calculated on the basis of 168,000 inch-pounds bending
moment, assuming no buckling of the longitudinals.

THE NORMAL RESTRAINT COEFFICIENT P/δ

The resistance of a stiffened cylinder to an exter-
nally applied radial load has been discussed in detail
in reference 3. As stated in the concluding remarks,
further experimental evidence was necessary to establish
the validity of P/δ as a correlation parameter for the
wire-braced and sheet-covered specimens. It was also
thought that this parameter might aid in predicting the
failing load of a specimen without applying any load to
the structure other than the loads necessary to obtain
the P/δ values. A plot of failing bending moment as
a function of P/δ for all the sheet-covered specimens
and for a number of the wire-braced specimens is shown
in figure 5. This plot indicates that the expected gen-
eral relationship does not hold, inasmuch as the failing
bending moment is not only a function of P/δ but also
varies with the longitudinal spacing. The linear re-
lationship, however, holds between certain limits. For
the sheet-covered specimens, the relation is linear with
the exception of the 1-inch frame spacing, which is an
extreme case and can hardly be expected to conform. For
the wire-braced specimens the relationship is, in general,
nonlinear. It should be noted that for the 5.06- and
10.12-inch longitudinal spacing the values of P/δ differ
by only a few percent. To investigate further the effect
of longitudinal spacing, the P/δ value was obtained for
a specimen in which the longitudinal spacing was 50.6
inches — that is, only the top and the bottom longitudinals
remained. The curves of P against δ for this specimen
and for a specimen having a 10.12-inch longitudinal spacing

are shown in figure 7. The difference in the initial slopes — that is, P/δ, is only 5 percent. The small difference which exists in the P/δ value as the spacing of the longitudinals is varied from 5.06 to 50.6 inches leads to the conclusion that after a certain longitudinal spacing, lying between 2.53 and 5.06 inches, P/δ is no longer a measure of the resistance of the specimen as a whole to an externally applied load but rather the resistance of a single longitudinal. The critical longitudinal compressive stress has also been plotted as a function of P/δ in figure 6. Only the sheet—covered specimens having a 2.53— and a 5.06—inch longitudinal spacing scatter around a common curve.

There are, therefore, two difficulties in using P/δ as a correlation parameter for the failing moment:

1. It is evident that the elastic characteristics of the stiffened cylinder are determined by the longitudinal and the circumferential stiffnesses. The measurement of P/δ gives only something like the mean stiffness in these two directions. If the failing moment is a function of the same mean stiffness, then the failing moment will be a function of P/δ only. If this is not true, then some other parameter like d/b (aspect ratio of stiffening) must be used with P/δ. This is confirmed by the experiments, as shown in figure 5.

2. It is also evident from figure 5 that the value of P/δ changes very slowly when the longitudinal spacing is large, while the failing moment changes very rapidly. Thus the failing moment against P/δ curve, at a constant d/b ratio, is very steep when the longitudinal spacing is large. Therefore, a small error in the P/δ determination gives a large error in the failing moment. It should, however, be kept in mind that the 10—inch longitudinal spacing is already considerably larger than that which would be encountered in practice for geometrically equal structures.

At present, there is no evidence of a reasonable correlation parameter between the sheet—covered and the wire—braced specimens, and it probably will be necessary to continue the experimental work with sheet—covered specimens.

DEFLECTION OF THE LONGITUDINALS

The deflection curves of the longitudinals, after
failure of the specimen, are shown in figures 17 to 34.
A marked difference has been observed in the type of
failure of the wire—braced and sheet—covered specimens.
Failure of the wire—braced specimens was in general a
gradual process — that is, the specimens tend to approach
a maximum bending moment in an asymptotic manner. The
failure, however, of the sheet-covered specimens is char—
acterized by a sudden and violent collapsing of the spec—
imen. The radial deflection of the longitudinals, for
longitudinal spacings less than 16 inches, is practically
zero up to the failing load. A number of photographs
(figs. 38 to 47) also are included to illustrate further
the failure pattern of the longitudinals and the frames.

EXPERIMENTAL INVESTIGATIONS ON COMPRESSIVE FAILING

STRESS OF UNSTIFFENED CIRCULAR CYLINDERS

In the discussion of the strength of axially loaded,
unstiffened cylinders (reference 1) it was pointed out
that a very poor agreement exists between experimental
results and those calculated by the classical buckling
theories for circular cylinders. This was especially
true for large values of R/t. It was also found that
very little information was available on the effect of
length, particularly for values of $L/R < 1$.

In view of the need for additional information con—
cerning those two parameters a systematic investigation
was carried out on steel cylinders in which the R/t
ratios were higher than had been previously investigated
and on cylinders whose lengths were less than the radius.
The specific parameters involved in this investigation
were:

1. the radius—thickness ratio R/t

2. the length—radius ratio L/R

3. the critical stress—elastic modulus ratio σ/E

The specimens tested were all fabricated from standard
shim stock steel in which the nominal thickness was
varied from 0.002 to 0.009 inch. Since the fabricated
cylinders had a radius of 6.375 inches the R/t range
varied from 750 to 3000. The L/R ratio was varied
from 0.1 to 1.5.

The ends of the test cylinder were rigidly clamped
into steel end plates, giving fixed end support to the
axial fibers of the cylinder. The test apparatus is
shown in figures 48 and 49. The load was applied by
means of the screw jack and transmitted through the ring,
which measures the load, to the cylinder. To prevent any
horizontal components of load, the ring was mounted on a
spherical ball joint.

The test results are shown in figures 35 and 36,
in which σ/E is plotted as a function of L/R for con-
stant values of R/t.

where

σ failing stress, pounds per square inch

E Young's modulus, pounds per square inch

An empirical equation was developed to fit the experimental
points. The equation is essentially of the same form as
the Wagner empirical design formula (reference 5), inasmuch
as the variables used are t/R and t/L; however, the co-
efficients and exponents have been modified to read:

$$\frac{\sigma}{E} = 9(t/R)^{1.6} + 0.16(t/L)^{1.3}$$

A plot of this equation for values of R/t and L/R
corresponding to the range of the experimental investi-
gation is shown by the curves in figures 35 and 36. For
values of L/R greater than 1.5 experimental results
indicate that σ/E is for all practical purposes a con-
stant.

These experimental results are again at variance
with the theoretical investigation of W. Flügge as cited
by S. Timoshenko. (See reference 1.) The classical theory
of W. Flügge shows that the length effect is negligible

until L/mR is lower than 0.2, where m is the number
of half—waves in the axial direction. Since the edges
of the test specimens were clamped, it is evident that
$m = 2$ for the short cylinders. According to the clas—
sical theory, therefore, the length effect is negligible
until L/R is less than 0.4. This is another failure
of the classical theory of thin shells to predict cor—
rectly the behavior of buckling phenomena.

Since the physical properties of the shim stock
varied for every thickness, it was necessary to deter—
mine experimentally the modulus of elasticity for each
thickness. The results are tabulated in table II. The
stress—strain relation was obtained for the material in
tension; the tension load was applied, with reference to
the grain structure of the material, in the same direction
as the compression load in the test cylinder.

DETAILED STUDY OF BUCKLING PHENOMENA

OF CYLINDRICAL SHELLS

The relatively large discrepancies between the theo—
retically predicted and the experimentally obtained buck—
ling loads have led to the conclusion that some of the
assumptions made in the theoretical treatment of the prob—
lem may be at variance with the actual conditions. Hence,
to obtain a better understanding of the mechanism involved
in the failure of thin-wall cylinders, it was felt that it
would be desirable to determine the exact shape of the
initial waves which appear in the test cylinder. This was
accomplished by restraining the loading mechanism so that
any desired over—all deflection could be maintained at
any stage of the loading.

The test apparatus is shown in figures 50 to 52.
The three upper set screws afford adjustment of the load—
ing head and rest on a 3/4—inch plate. This plate, in
turn, is held in position by three 1/2—inch screws rest—
ing on the base plate and turned by means of the gear
system shown. This lowers or raises the 3/4—inch plate
as desired. The small 2—inch central gear, which turns
the three 5—inch diameter gears, can be externally operated.
In this manner the motion of the loading head can be arrest—
ed at any desired position during loading of the specimen.

The progressive change in the wave shape and the wave pattern is indicated in figures 53 to 64. The first specimen, designated as C-1 to C-6 in the figures, was 9 inches long with a 0.0034-inch wall thickness. The second specimen, C-8 to C-13, was 6 inches long with a 0.0034-inch wall thickness.

It should be noted that the wave pattern does not agree with the uniformly distributed sinusoidal type of wave which has been previously assumed for the theoretical solution. The initial wave form is elliptical in shape and scattered at random through the specimen. As the load is increased, the waves tend toward a diamond shape and move to a more uniform configuration. The discrepancy between the actual and the assumed wave form may account for the large difference in the theoretically predicted and the experimentally obtained buckling load.

Guggenheim Aeronautical Laboratory,
        California Institute of Technology,
                Pasadena, Calif., September 1939.

REFERENCES

1. Guggenheim Aeronautical Laboratory, California Institute of Technology: Some Investigations of the General Instability of Stiffened Metal Cylinders I — Review of Theory and Bibliography. T.N. No. 905, NACA, 1943.

2. Guggenheim Aeronautical Laboratory, California Institute of Technology: Some Investigations of the General Instability of Stiffened Metal Cylinders II — Preliminary Tests of Wire-Braced Specimens and Theoretical Studies. T.N. No. 906, NACA, 1943.

3. Guggenheim Aeronautical Laboratory, California Institute of Technology: Some Investigations of the General Instability of Stiffened Metal Cylinders. III — Continuation of Tests of Wire-Braced Specimens and Preliminary Tests of Sheet-Covered Specimens. T.N. No. 907, NACA, 1943.

4. Cox, H. L.: Stress Analysis of Thin Metal Construction. R.A.S., vol. XLIV, March 1940.

5. Ballerstedt, W., and Wagner, H.: Versuch über die Festigkeit dünner Unversteifter Zylinder. Luftfahrtforschung, 1936, p. 309.

TABLE I

PURE BENDING TESTS OF LONGITUDINALS – FRAME COMBINATIONS

[All longitudinals S_1; all frames F_5]

Test	Longitudinal spacing, b (in.)	Frame spacing, d (in.)	Number of frames in 64 in.	P/δ	Failing moment M.B. (in.-lb)	Max. compressive stress at failure	Type of failure
25	2.53	8	7	330	219,000	16,200	General instability..
26	2.53	4	15	450	274,000	19,400	Do.
27	2.53	2	31	614	359,000	25,600	Do.
28	2.53	16	3	255	168,500*	13,000	Started by panel instability – final failure general instability.
29	5.06	16	3	222	123,000*	6,600**	Panel instability.
30	5.06	8	7	257	107,500	12,200	General instability.
31	5.06	4	15	350	137,500	16,500	Do.
32	5.06	2	31	510	185,000	22,200	Do.
34	10.12	16	3	209	50,000	8,200	Started by panel instability – final failure general instability.
35	10.12	8	7	261	60,000	10,500	General instability.
36	10.12	4	15	361	75,000	14,200	Do.
37	10.12	2	31	476	100,000	17,800	Do.
38	5.06	1	63	740	209,000	26,000	Do.
39	2.53	1	63	815	397,000	29,600	Do.

*Failing bending moment.
**Panel instability stress.

TABLE II

VARIATIONS OF YOUNG'S MODULUS

WITH THICKNESS

Nominal thickness (in.)	Young's modulus (lb/sq in.)
0.002	33.5×10^{6}
.003	32.0
.004	32.4
.005	31.5
.006	30.6
.0085	29.0

TABLE III

CALCULATION OF CRITICAL STRESS BY RYDER'S METHOD

FOR SHEET-COVERED SPECIMENS

Spec-imen	Longi-tudinal spacing, b (in.)	Frame spac-ing d (in.)	Max. com-pressive stress at failure, $(\sigma_{cr})_{exp}$	$\dfrac{\sigma_{cr}}{\sigma_b}$	$\dfrac{I_{\sigma f}/I_{of}}{I_{\sigma l}/I_{ol}}$	K_1	$K_2 = \dfrac{I_{\sigma f}b}{K_1 I_{\sigma l}d}$	$\dfrac{A_{\sigma f}}{A_{\sigma l}}$	$K_3 = \dfrac{A_{\sigma f}b}{K_1 A_{\sigma l}d}$	$K_4 = \dfrac{G'tb}{EK_1 A_l}$	t_o/ρ_l (from Ryder's curves)	Calcu-lated criti-cal stress (lb/sq in.)
27	2.53	2	25,600	6.40	1.29	1.30	0.0541	0.915	0.894	0.101	0.50	22,290
26	2.53	4	19,400	5.88	1.29	1.30	.0270	.922	.448	.100	.30	13,380
25	2.53	8	16,200	5.40	1.30	1.30	.0135	.917	.223	.100	.18	8,410

NOTE:

All figures are four times actual size

028"

.320"

x   X

.420"
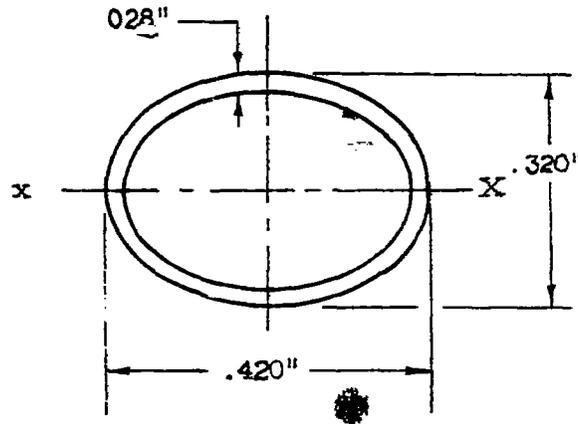
STIFFENER - S_1

AREA = .0324 sq.in. I_{xx}=.000374 in.^{4}

x   x .0796"

.366"
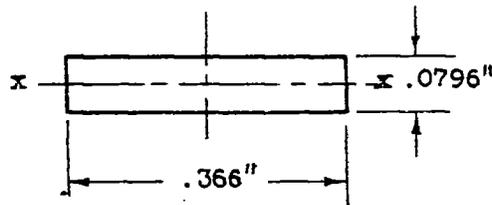
FRAME - F_5

AREA =.0291 sq.in. I_{xx} =1.557 x 10^{-5}

FIGURE 1
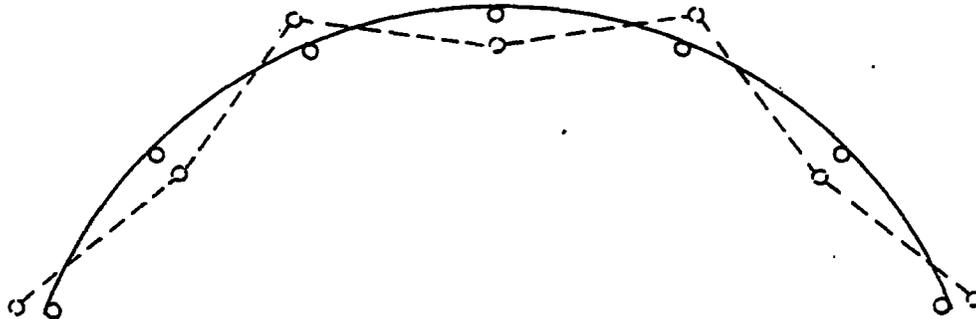
FIGURE 2

Deflection pattern of longitudinals causing transverse
stresses to be set up in the sheet.

FIGURE 3

Diagram showing measurement of overall axial deflection.

CRITICAL LONGITUDINAL STRESS AS A FUNCTION OF THE LONGITUDINAL SPACING - b FOR CONSTANT VALUES OF d/b

FIG. 4

FAILING BENDING MOMENT
AS A FUNCTION OF P/δ
AT ZERO BENDING MOMENT

RADIUS OF CYLINDER 15.76"

LINES OF CONSTANT
ASPECT RATIO d/b

FAILING BENDING MOMENT × 10^{-3} ~ INCH LBS.

2.53" LONGITUDINAL SPACING
5.06" " "
10.12" " "
WIRE BRACING

NORMAL RESTRAINT COEFFICIENT ~ $\frac{P}{\delta}$ ~ LBS/INCH

FIG 5

Fig. 5

Fig. 6

FAILING COMPRESSIVE STRESS ~ LBS./SQ.INCH

NORMAL RESTRAINT COEFFICIENT ~ P/δ ~ LBS./INCH

2.53" LONGITUDINAL SPACING

5.06"   "   "

10.12"   "   "

WIRE BRACING

SHEET COVERING

Fig. 6

RADIAL DEFLECTION
AS A FUNCTION OF
APPLIED LOAD - P

TESTS #36 & #36A

o 10" LONGITUDINAL SPACING
+ 50" " "

4" FRAME SPACING
FOR BOTH

LOAD IN LBS

RADIAL DEFLECTION IN INCHES

FIG 7

Fig. 7

MAXIMUM LONGITUDINAL STRESS
AS A FUNCTION OF
BENDING MOMENT

TEST #27

o—o TENSION
△—△ COMPRESSION

BENDING MOMENT ~ INCH – LB

MAXIMUM LONGITUDINAL STRESS ~ LBS./SQ. INCH

FIG. 8

MAXIMUM LONGITUDINAL STRESS - TEST #32
AS A FUNCTION OF
BENDING MOMENT

BENDING MOMENT ~ INCH LBS.

MAXIMUM LONGITUDINAL STRESS - LBS/SQ. INCH

o—o TENSION
▲—▲ COMPRESSION

FIG. 9

MAXIMUM LONGITUDINAL STRESS AS A FUNCTION OF BENDING MOMENT

FIG 10

FIG. 11

MAXIMUM LONGITUDINAL STRESS
AS A FUNCTION OF
BENDING MOMENT

TEST # 39

TENSION
COMPRESSION

BENDING MOMENT ~ INCH LBS.

MAXIMUM LONGITUDINAL STRESS ~ LBS./SQ.INCH.

FIG. 12

TEST #25

STRESSES IN THE LONGITUDINALS
AS A FUNCTION OF THE APPLIED
BENDING MOMENT

o—o INSIDE
o—o OUTSIDE

FIG. 13

Fig. 14

Fig. 14

TEST #25
STRESSES IN THE LONGITUDINALS
AS A FUNCTION OF THE APPLIED
BENDING MOMENT

INSIDE
OUTSIDE

BENDING MOMENT IN INCH LBS

STRESS IN LBS/SQ INCH

Fig. 16

Fig. 15

Fig. 16

FIG. 16

Test #35
Frame #5

Station #4

Station #8

RADIAL DEFLECTION
AT FAILURE
40 LONGITUDINALS
7 FRAMES

Station #12

Station #16

Station #18

Fig 17

Test #25
Frame #5

Radial Deflection at Failure
40 Longitudinals
7 Frames

Station #18   Station #20

Station #25   Station #30

Fig. 18

Fig. 19

Fig 19

Fig. 20

Fig. 20

TEST 26
DEFLECTION OF LONGITUDINALS
40 LONGITUDINALS

Fig. 31

TEST "26
DEFLECTION OF LONGITUDINALS
40 LONGITUDINALS

FRAMES

Fig. 22

Fig. 23

Test #27
Deflection of Longitudinals
40 Longitudinals

Fig 23

Fig. 24

TEST #28
DEFLECTION OF LONGITUDINALS
40 LONGITUDINALS

FIG. 24

TEST 29 — DEFLECTION OF LONGITUDINALS — 20 LONGITUDINALS

FIG. 25

Fig. 26

Test #30
Deflection of Longitudinals
10 Longitudinals

Fig. 26

Test #31
Deflection of Longitudinals
20 Longitudinals

Fig 27

Test #32
Deflection of Longitudinals
20 Longitudinals

$\gamma = 36°$

Frames

10"

$\gamma = 18°$

$\gamma = 0°$

$\gamma = 324°$

10"

$\gamma = 342°$

64"

Fig. 28

TEST #33
DEFLECTION OF LONGITUDINALS
20 LONGITUDINALS

Fig. 29

TEST #34
DEFLECTION OF LONGITUDINALS
10 LONGITUDINALS

FIG 30

FIG. 31

Fig. 32

TEST #36
DEFLECTION OF LONGITUDINALS
10 LONGITUDINALS

FIG. 32

Fig. 33

NACA Technical Note No. 908

TEST #37
DEFLECTION OF LONGITUDINALS
10' LONGITUDINALS

FIG. 33

TEST #38
DEFLECTION OF LONGITUDINALS
20 LONGITUDINALS

ONE INCH FRAME SPACING

γ=36°

1.0"

γ=18°

γ=0°

γ=342°

10"

γ=324°

64"

FIG 34

Fig. 35

COMPRESSION TEST OF CIRCULAR CYLINDERS

LENGTH EFFECT

$\frac{\sigma}{E}$ VS. $\frac{L}{R}$

EXPERIMENTAL POINTS
WITH EMPERICAL
DESIGN FORMULA

$$\frac{\sigma}{E} = 9\left(\frac{t}{R}\right)^{1.6} + .16\left(\frac{t}{L}\right)^{1.3}$$

LIMITS $0.1 < \frac{L}{R} < 1.5$
FOR $\frac{L}{R} > 1.5$ ASSUME CONSTANT

$\frac{R}{t}$

FAILING STRESS / ELASTIC MODULUS

$\frac{\sigma}{E} = \eta$

750

1250

2000

3000

$\frac{L}{R} = \frac{LENGTH}{RADIUS}$

FIG. 35

COMPRESSION TEST OF CYLINDERS

LENGTH EFFECT

$$\frac{\sigma}{E} \text{ vs. } \frac{L}{R}$$

EXPERIMENTAL POINTS
WITH EMPERICAL
DESIGN FORMULA

$$\frac{\sigma}{E} = 9\left(\frac{t}{R}\right)^{1.6} + .16\left(\frac{t}{L}\right)^{1.3}$$

LIMITS $0.1 \leq \frac{L}{R} \leq 1.5$

FOR $\frac{L}{R} > 1.5$ ASSUME CONSTANT

$\frac{\sigma}{E} = \frac{\text{FAILING STRESS}}{\text{ELASTIC MODULUS}}$

$\frac{R}{t}$

1000

1500

0 .1 .2 .3 .4 .5 .6 .7 .8 .9 1.0

$$\frac{L}{R} = \frac{\text{LENGTH}}{\text{RADIUS}}$$

.00100
.00090
.00080
.00070
.00060
.00050
.00040
.00030
.00020
.00010
.00005

Fig. 36

Fig. 37

Fig. 38

Fig. 39

Fig. 40

Fig. 41

Fig. 42

Fig. 43

Fig. 44

Fig.45

Fig. 46

Fig. 47

Fig. 49
Assembled Cylinder

Fig. 48
Test Apparatus with
Specimen in Position.

Fig. 50
Head Lowering
Mechanism.

Fig. 51
Gear System

Fig. 52
Loading Apparatus

Fig. 53

Fig. 54

Fig. 55

Fig. 56

Fig. 57
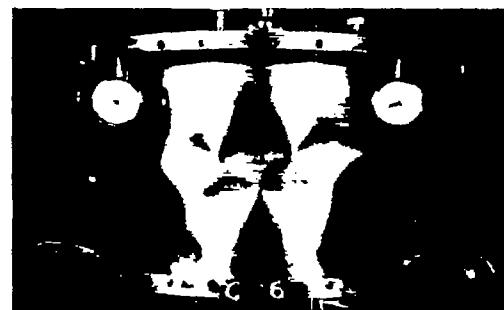
Fig. 58
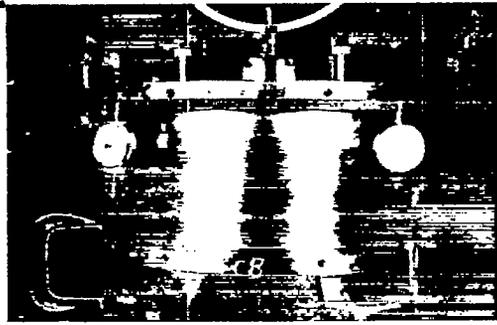
Fig. 59
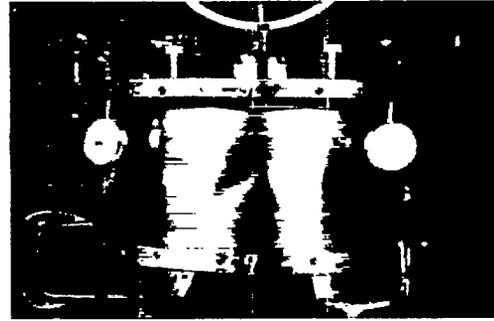
Fig. 60

Fig. 61

Fig. 62

Fig. 63

Fig. 64